Bollettino di Geofisica Teorica ed Applicata Vol. 55, n. 3, pp. 617-639; September 2014
DOI 10.4430/bgta0117

Time dependent seismicity in the continental fracture system

B.C. Papazachos, G.F. Karakaisis and E.M. Scordilis

Dept. of Geophysics, School of Geology, Aristotle University, Thessaloniki, Greece

(Received: October 4, 2012; accepted: September 24, 2013)

ABSTRACT Two time-dependent seismicity models are tested by using recent reliable data of earthquakes generated in active regions of ten large areas (West Mediterranean, Aegean, Cyprus, Anatolia, Central Asia, Sumatra-Java, Japan, North Pacific, California, South America) of the continental fracture system. The first one, called TIMAPR (Time and Magnitude Predictable Regional) model is based on interevent times of strong mainshocks (M=6.3-9.0) generated in circular seismogenic regions (networks of faults). The second, called D-AS (Decelerating-Accelerating Seismicity) model, is based on triggering of a mainshock by its preshocks. Tests of decelerating-accelerating precursory seismicity against synthetic catalogues with spatio-temporal clustering verify the validity of the D-AS model. Backward tests of both models showed that: a) every strong shallow mainshock is preceded by a decelerating and an accelerating preshock sequence within well-defined time, space and magnitude windows, allowing its intermediate-term prediction by the D-AS model, and b) in each circular seismogenic region the mainshocks show quasi-periodic behavior with interevent times following the TIMAPR model which is also applied to predict the mainshock. Forward tests of both models indicate candidate regions for the generation of strong mainshocks during the next decade (2013-2022 or so). Estimated (predicted) values of their basic focal parameters (time, magnitude, epicenter) and their uncertainties are given to objectively define the predicting ability of the joint application of the two models.

Key words: time-dependent seismicity, TIMAPR, D-AS, preshocks.

1. Introduction

We examine the time-dependent seismicity along the two large seismic zones of the continental fracture system, i.e. the Mediterranean-Central Asia-Indonesia zone and the circum-Pacific zone, where lithospheric convergence takes place and where most of the shallow (h≤100 km) and all deep global seismic activity occur along these two large seismic zones. We used data concerning recent earthquakes generated in very active circular regions (seismogenic regions) which are located in the following ten areas of these two large zones: 1) West Mediterranean, 2) Aegean, 3) Cyprus, 4) Anatolia, 5) Central Asia, 6) Sumatra-Java, 7) Japan, 8) North Pacific, 9) California, 10) South America. These data are used to check the validity of two time-dependent seismicity models. The first of these models is the Time and Magnitude Predictable Regional (TIMAPR) model, which is based on interevent times of strong mainshocks generated in a region of very active faults (Papazachos *et al.*, 1997, 2010a, 2011). The second model

is the Decelerating-Accelerating Seismicity (D-AS) model which is based on triggering of a mainshock by its preshocks (Papazachos *et al*., 2006b, 2010a, 2011).

A homogeneous (in respect to magnitude) earthquake catalogue for the entire continental fracture system was compiled spanning more than a century (1.1.1900-31.10.2011), with completeness defined separately for each one of the ten areas. Data sources searched to compile this catalogue are the bulletins of the International Seismological Centre (ISC, 2012), the National Earthquake Information Centre of USGS (NEIC, 2012), the online Global Moment Tensor Catalogue (GCMT, 2012) and published global earthquake catalogues (Pacheco and Sykes, 1992; Engdahl and Villaseñor, 2002). Magnitudes in these data sources are given in several scales (M_s, m_b, M_L, M_{JMA}, M_w). To ensure homogeneity of the catalogue in respect to the magnitude, all magnitudes were transformed into the moment magnitude scale M_w(=M) by appropriate formulas (Scordilis, 2005, 2006). The finally adopted magnitude for each earthquake is either the original moment magnitude (published by Pacheco and Sykes, 1992; GCMT, 2012; NEIC, 2012) or the equivalent moment magnitude estimated as the weighted mean of the converted magnitude values by weighting each participating magnitude with the inverse standard deviation of the respective relation applied. Typical errors of the catalogue are up to 0.3 for the magnitude and up to 30 km for the locations, which are satisfactory for the purposes of the present work. Fig. 1 shows the epicenters of all known strong (M≥7.0) earthquakes that occurred in the continental fracture system between 1.1.1900 and 31.10.2011.

In this paper, after describing briefly the basic principles and the recently improved procedures for predicting mainshocks by the two models (sections 2 and 3), we present in section 4 the results of backward tests of both models with the aim of testing the validity of the two models by recent reliable global data and of estimating (retrospectively predicting) the main parameters of already occurred recent mainshocks. We also attempt predictions of probably ensuing mainshocks during the next decade or so in seismogenic regions of each one of the ten areas examined (section 5). The last section (6) includes the conclusions and discussion.

2. The TIMAPR model

This model was developed in the 1990s on the basis of a large sample of global data concerning mainshocks that occurred in an equally large number of seismogenic regions (Papazachos *et al.,* 1997). Additional data of recent strong mainshocks (M=6.3-9.0) augmented the available global sample thus contributing to the model's improvement [see for details Papazachos *et al*. (2010a, 2011)]. Basic information for the model is given below along with the improved relations used for prediction of ensuing mainshocks.

2.1. Basic information on the model

The available large sample of global data (interevent times of mainshocks located in each seismogenic region, etc.) was used to derive two relations of the form:

$$\log T_t = bM_{\min} + cM_p + d \log S_d + q \quad (1)$$

$$M_f = BM_{\min} + CM_p + D \log S_d + w \quad (2)$$

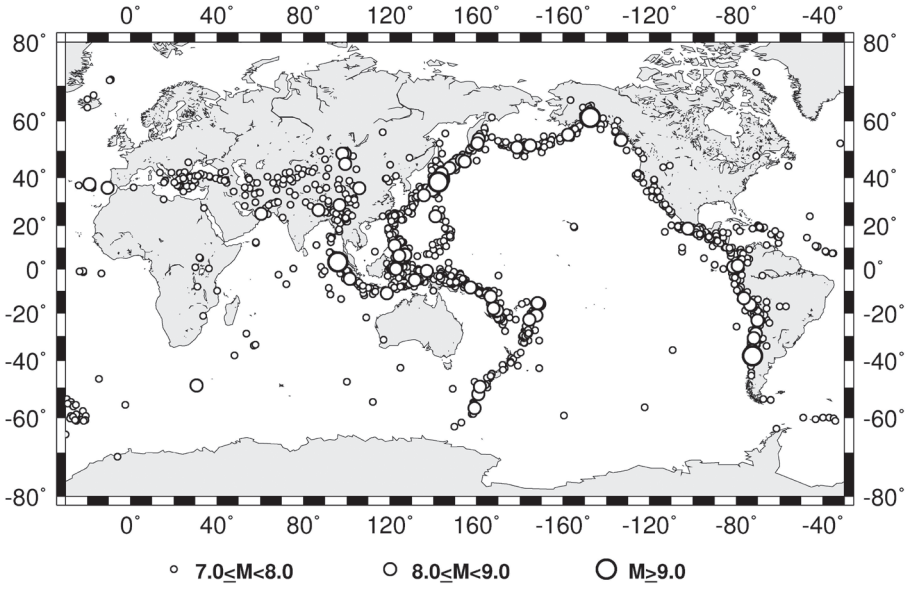

Fig. 1 - Epicenters of strong (M≥7.0) shallow earthquakes which occurred during the instrumental period (1900-2011) in the two seismic zones (Mediterranean-Indonesian, circum-Pacific) of the continental fracture system, where the ten areas, examined in the present work, are located (1. West Mediterranean, 2. Aegean, 3. Cyprus, 4. Anatolia, 5. Central Asia, 6. Sumatra-Java, 7. Japan, 8. North Pacific, 9. California, 10. South America). The three sizes of open circles correspond to three ranges of moment magnitudes.

where T_t (in years) is the interevent time, M_{min} is the minimum mainshock magnitude of the seismogenic region, M_p and M_f are the magnitudes of the previous and the following mainshock, respectively, S_d (in Joules$^{1/2}$ per year) is the seismic strain rate in the seismogenic region and q, w are constants. The available sample of data (T_t, M_{min}, M_p, M_f, S_d) was used to calculate the values of the scaling coefficients (b=0.19, c=0.33, d=-0.54, B=0.73, C=-0.28, D=0.46) which are of global validity. The average values of the constants q and w and the corresponding standard deviations (σ_q, σ_w) are calculated by the available data for each examined seismogenic region.

It has been also shown that the ratio T/T_t of the observed interevent time, T, to the calculated, T_t [by Eq. (1)], follows a lognormal distribution with a mean equal to zero and a standard deviation, σ (Papazachos and Papaioannou, 1993). This property allows the calculation of the probability, $P(\Delta t)$, for the occurrence of a mainshock with $M \geq M_{min}$ during the next Δt years, if the previous mainshock ($M_p \geq M_{min}$) occurred in the region t years ago. This is done by the relation:

$$P(\Delta t) = \frac{F(L_2/\sigma) - F(L_1/\sigma)}{1 - F(L_1/\sigma)} \tag{3}$$

where $L_2 = \log\frac{t+\Delta t}{T_t}$, $L_1 = \log\frac{t}{T_t}$ and F is the complementary cumulative value of the normal distribution with mean equal to zero and standard deviation, σ. T_t is calculated by Eq. (1), since M_{min}, M_p, $\log S_d$ and the scaling coefficients (b, c, d) are known. The constant, q, and its standard deviation for each seismogenic region are also known.

2.2. Compilation of a catalogue of mainshocks

The basic Eqs. (1), (2) and (3) of the TIMAPR model hold for the mainshocks of each seismogenic region which is assumed circular in the present work. The seismogenic region is defined by the distribution of the foci of decelerating preshocks (see section 3.1). The mainshocks in this region behave as the characteristic earthquakes (Schwartz and Coppersmith, 1984) in a seismic fault. That is, the mainshocks generated in a seismogenic region do not obey the G-R frequency-magnitude linear relationship (which applies for the smaller shocks of the region) but their interevent times have a quasi-periodic behaviour and follow Eq. (1). Hence, it is necessary to decluster properly the original (complete) earthquake catalogue, that is, to identify and remove all associated shocks (not only those that occur on the mainshock fault a few days to weeks before and after its rupture [foreshocks, aftershocks] but also other shocks that occur in the seismogenic region [preshocks, postshocks] up to several years before and after the mainshock occurrence). For this reason, a minimum mainshock magnitude, M_{mp}, and an appropriate time window, Δt, must be defined.

The proper minimum mainshock magnitude of an area depends on the maximum magnitude level of the generated earthquakes in the area. Thus, for areas with maximum magnitude level M~7.5 (e.g. Mediterranean, California) the minimum mainshock magnitude can be M_{mp}=6.5, and for areas with maximum magnitude level M>7.5 (Japan, N. Pacific, etc.) the minimum mainshock magnitude can be M_{mp}=7.0.

The optimum time window is defined by the ratio σ/T, where T is the mean interevent time and σ its standard deviation, because this ratio is a measure of seismic clustering and for σ/T <0.50 an earthquake catalogue exhibits quasi-periodic behavior (Kagan and Jackson, 1991). By using data of globally occurred earthquakes, it has been shown that for $\Delta t \geq 15.0$ years this ratio becomes smaller than 0.50 and remains almost constant (~0.35) with increasing Δt. For this reason, the declustering window is taken equal to Δt=15.0 years. The validity of this result has been confirmed (see section 4.1) by using the relative data concerning the seismogenic regions of the twenty globally occurred mainshocks listed in Table 1. The catalogue of mainshocks in a seismogenic region, with quasi-periodic properties, results from the application of the following declustering scheme on the original (complete) catalogue of earthquakes of the region.

The largest earthquake of the available complete sample for a seismogenic region is considered as the first mainshock of the region. The first mainshock and its associated shocks (shocks of the original catalogue of the region that occurred within a time window ±15.0 years from the origin time of their mainshock) are excluded from the original catalogue. Then, the largest earthquake of the remaining (residual) catalogue is considered as a mainshock and its associated shocks, defined in the same way as previously, are also excluded from the first residual catalogue, and so on till no earthquake with $M \geq M_{mp}$ remains in the final residual catalogue. In this way a mainshock catalogue is created for the seismogenic region examined.

2.3. Prediction by the TIMAPR model

For prediction by this model of the origin time, the magnitude and the epicenter coordinates of an ensuing mainshock in a predefined seismogenic region the following procedure is applied: The origin time, t_t, is calculated by the empirical relation based on global data:

$$t_t - t_f^* = 40.1 P_f^* - 22.3 \qquad (4)$$

Table 1 - Information on the retrospective predictions of the two last strong ($M \geq 6.3$) mainshocks occurred in each one of the ten areas the names of which are written in the first column of the table. The t_c, M and $E(\phi,\lambda)$ are the observed origin times, magnitudes and epicenter coordinates of these twenty mainshocks, t_t and M_t are the retrospectively predicted by the TIMAPR model, origin time and magnitude, and t_d, M_d are the retrospectively predicted by the D-AS model, origin time and magnitude. t_c^* and M^* are the finally adopted as predicted origin time and magnitude (mean values of the corresponding values calculated by the two models). $E^*(\phi,\lambda)$ are the geographic coordinates of the retrospectively predicted epicenters based on both models.

Area	t_c	M	$E(\phi,\lambda)$	t_t	M_t	t_d	M_d	t_c^*	M^*	$E^*(\phi,\lambda)$
W. Mediterranean	2003:05:21 2004:02:24	6.8 6.4	36.9, 3.8 35.3, - 4.0	2004.2 1999.1	6.9 6.5	2003.8 2004.0	6.8 6.4	2004.0 2001.6	6.9 6.5	36.1, 3.5 36.6, -4.6
Aegean	2008:02:14 2009:07:01	6.7 6.4	36.8, 21.7 34.2, 25.5	2009.0 2011.3	7.6 7.8	2007.9 2008.7	6.8 6.4	2008.5 2010.0	7.2 7.1	37.0, 21.3 35.5, 25.5
Cyprus	1996:10:19 1998:06:27	6.8 6.3	34.5, 32.1 36.8, 35.3	1990.5 1994.3	7.1 7.5	1996.4 1999.2	6.7 6.3	1993.5 1996.8	6.9 6.9	36.2, 32.2 38.2, 35.1
Anatolia	1999:08:17 2011:10:23	7.5 7.2	40.8, 30.0 38.7, 43.5	1996.9 2012.8	7.8 7.4	1999.0 2012.6	7.3 7.2	1998.0 2012.7	7.6 7.3	40.8, 27.6 38.5, 43.7
Central Asia	2008:03:20 2011:01:18	7.2 7.2	35.5, 81.5 28.7, 63.9	2005.0 2003.6	7.4 7.3	2007.7 2011.0	7.2 7.2	2006.4 2007.3	7.3 7.3	35.1, 82.3 28.7, 61.9
Sumatra	1994:06:02 2004:12:26	7.8 9.0	-10.4, 112.9 03.4, 95.9	1988.3 2001.3	7.9 8.3	1993.6 2004.8	7.5 8.7	1991.0 2003.1	7.7 8.5	-10.8, 113.5 02.1, 96.7
Japan	2003:09:28 2011:03:21	8.3 9.0	41.8, 143.9 38.3, 142.4	2007.2 2009.9	8.5 8.8	2003.0 2011.0	8.4 8.7	2005.1 2010.5	8.5 8.8	41.6, 142.3 37.0, 141.0
N. Pacific	2003:11:17 2006:11:15	7.7 8.1	51.1, 178.6 46.7, 153.2	2004.5 2006.6	8.4 8.5	2004.3 2007.3	7.8 8.1	2004.4 2007.0	8.1 8.3	51.4, 179.2 46.1, 152.5
California	2010:01:10 2010:04:04	6.5 7.1	40.6, -124.8 32.1, -115.2	2005.8 2010.6	7.4 7.1	2011.0 2012.4	6.7 7.1	2008.4 2011.5	7.1 7.1	40.0, -123,2 32.7, -116.2
S. America	2001:06:13 2010:02:27	8.3 8.8	-16.3, -73.6 -36.5, -73.2	2004.3 2011.4	8.4 9.0	2001.4 2010.4	7.9 8.6	2002.9 2010.9	8.2 8.8	-17.3, -72.9 -35.9, -72.7

where, t_f^* is a preliminary predicted origin time (given by the relation $t_f^*=t_p+T_t$) and P_f^* is the probability [given by the Eq. (3), for t= t_f^*-5.0 years and Δt=10.0 years].

The magnitude, M_t, of the ensuing mainshock is given by Eq. (2).

The TIMAPR model also contributes to the location of an ensuing mainshock, because the geographic mean, L, of the epicenters of all known past mainshocks located in the seismogenic region, is one of the two geographic points used to locate (predict) the epicenter of the ensuing mainshock (see section 3.1).

There are cases where the available complete instrumental data for a circular seismogenic region are not enough for application of the TIMAPR model (such cases are mainly observed in low seismicity areas). In these cases historical data are also used, if such data are available, but if not, then the radius of the seismogenic region increases in steps till the available instrumental data allow the application of the model (e.g. till the number of the interevent times between mainshocks becomes at least 3).

3. The D-AS model

This model has been developed during the last decade and is explained in detail in published papers (Papazachos *et al*., 2006b, 2010a, 2011). Basic properties of the model are described and improved relations used for prediction of mainshocks are given in this section.

3.1. Basic information on the model

The D-AS model is based on predictive properties of seismicity which preceded each of 67 strong (M=6.3-9.0) earthquakes which form seven complete samples of mainshocks generated recently (since 1980) in a variety of seismotectonic regimes (28 in Mediterranean, 9 in Central Asia, 2 in Sumatra, 6 in Japan, 6 in North Pacific, 12 in California, 4 in S. America). Most of the data of this work can be found in Papazachos *et al*. (2006b). Observations on the precursory seismic activity of these mainshock samples indicate that every shallow ($h \leq 100$ km) strong ($M \geq 6.3$) mainshock is preceded by a sequence of smaller shocks which release decelerating with time seismic strain (decelerating preshocks) and shocks which release accelerating with time seismic strain (accelerating preshocks). Both sequences (accelerating, decelerating) follow the power-law relation:

$$S(t) = A + B\,(t_c - t)^m \tag{5}$$

where S (in Joule$^{1/2}$) is the cumulative Benioff strain (sum of square root of seismic energy), t is the time to the mainshock, t_c is the origin time of the mainshock and A, B, m are parameters calculated by the available data for each region (Bufe and Varnes, 1993), with $m<1$ for accelerating preshocks and $m>1$ for decelerating preshocks.

Decelerating and accelerating preshocks of a mainshock do not occur in the same space, time and magnitude windows. Decelerating preshocks occur in a narrow region (seismogenic) close to the mainshock epicenter whereas accelerating preshocks occur in a broader (critical) region. The seismogenic and the critical regions are both assumed circular in the present work. The minimum magnitude of decelerating preshocks of a mainshock with magnitude M (calculated by the relation $M_{min}=0.29\cdot M+2.35$) is smaller than the minimum magnitude of its accelerating preshocks (calculated by the relation $M_{min}=0.46\cdot M+1.91$). An accelerating seismic sequence starts earlier ($t_{sa}<t_{sd}$) and usually ends later than the corresponding decelerating one.

The generation of accelerating preshocks is considered as a critical phenomenon which leads to the triggering of the mainshock (Tocher, 1959; Sykes and Jaumé, 1990; Sornette and Sammis, 1995; Knopoff *et al*., 1996; Brehm and Braile, 1999; Robinson, 2000; Tzanis *et al*., 2000; Rundle *et al*., 2000; Papazachos *et al*., 2005a; Mignan *et al*., 2006, among others). Deceleration of strain in the seismogenic region is attributed to the break of the largest faults of this region during the first (excitational) phase which is inevitably followed by quiescence of strain release. This is supported by a frictional stability model (Gomberg *et al*., 1998) which explains in this simple way seismic quiescence that follows seismic excitation. The generation of preshocks in the seismogenic region contributes much to triggering of the mainshock due to their large magnitude during the first (excitational) phase, to their large number, manifested by the relatively large (>1.0) b-value (Helmstetter, 2003) during the second phase and to their geographical proximity to the focal region of the mainshock.

In an attempt to quantify strain acceleration Papazachos *et al*. (2002) proposed the index, $q_{a,}$ which is given by the relation:

$$q_a = \frac{P_a}{m_a C_a} \tag{6}$$

where, m_a is the power-law exponent of Eq. (5), with values between 0.25 and 0.35 that are in agreement with previous results (e.g. Ben-Zion and Lyakhovsky, 2002), C_a is the curvature parameter defined by Bowman *et al*. (1998) as the ratio of the *rms* error of the power-law fit [Eq. (5)] to the corresponding linear fit error and P_a is the probability that an accelerating seismic sequence fulfils the following relations based on global data (Papazachos *et al*., 2006b):

$$\log R = 0.42M - 0.30 \log s_a + 1.25, \qquad \sigma = 0.16 \tag{7}$$

$$\log (t_c - t_{sa}) = 4.60 - 0.57 \log s_a, \qquad \sigma = 0.17. \tag{8}$$

In these two relations, R (in km) is the radius of the circular region (critical region) where the epicenters of the accelerating preshocks are located, M is the mainshock magnitude, s_a is the Benioff strain release rate (in $J^{1/2}/10^4\,km^2\,yr$) in the critical region and t_{sa} is the start time (in years) of the accelerating seismic sequence.

Similarly, Papazachos *et al*. (2005b) defined the strain deceleration index, q_d:

$$q_d = \frac{P_d \cdot m_d}{C_d} \tag{9}$$

where m_d is the power in Eq. (5) with values ranging between 2.5 and 3.5, C_d is the curvature parameter for the decelerating seismicity and P_d is the probability that a decelerating seismic sequence fulfils the global relations:

$$\log a = 0.23M - 0.14 \log s_d + 1.40, \qquad \sigma = 0.15 \tag{10}$$

$$\log (t_c - t_{sd}) = 2.95 - 0.31 \log s_d, \qquad \sigma = 0.12 \tag{11}$$

where a (in km) is the radius of the circular region where the epicenters of the decelerating preshocks are located (seismogenic region), s_d is the Benioff strain release rate in this region (in $J^{1/2}/10^4\,km^2\,yr$) and t_{sd} is the start time of the decelerating seismic sequence. Observations on global data resulted in the following cut-off values of the parameters that describe the accelerating and the decelerating sequences, respectively:

$$C_a \le 0.70, \quad P_a \ge 0.45, \quad q_a \ge 2.00, \quad 0.25 \le m_a \le 0.35 \tag{12}$$

$$C_d \le 0.60, \quad P_d \ge 0.45, \quad q_d \ge 3.00, \quad 2.5 \le m_d \le 3.5 \tag{13}$$

Both indexes q_d and q_a are very useful in searching for decelerating and accelerating

precursory sequences related to a mainshock since they are indicative of the quality of the solutions, because they have their largest values (from global data: q_{df}=8.6±2.7, q_{aq}=8.0±2.5) at the seismogenic and the critical region, respectively. These quality indexes vary with time [see Fig. 2 in Papazachos *et al*. (2007a)], attaining their largest values a few years before the mainshock occurrence. They also vary in space since the geographical point with the highest q_d value corresponds to the center, *F*, of the seismogenic region, which is close to the mainshock epicenter, *E* (*FE*=220±60 km), whereas the geographical point where the largest q_a value is found corresponds to the center, *Q*, of the broader critical region (*QE*=350±150 km) where accelerating preshocks are generated (Karakaisis *et al*., 2007, 2013). This observation facilitates the identification of the critical region [see Fig. 10 in Papazachos *et al*. (2005a)] since problems have been reported when optimization procedures for defining this region are based solely on the values of the curvature parameter *C* (Mignan, 2008). Decelerating and accelerating sequences are hardly recognizable in circular regions centered at the mainshock epicenter (low q_d and q_a values), in accordance with the results of Hardebeck *et al*. (2008) after tests on synthetic earthquake catalogues.

3.2. Prediction by the D-AS model

Eqs. (8) and (11) are used to calculate (predict) the origin time, t_c, of the mainshock which is the average of the two values calculated by these equations. The magnitude, *M*, of this mainshock is the mean value of magnitudes calculated by the Eqs. (7) and (10).

The location of the epicenter, $E(\phi,\lambda)$, of an ensuing mainshock is based on properties of decelerating preshocks and on the location of previously occurred large mainshocks. In particular, as predicted epicenter of an ensuing mainshock is considered the geographic mean (mean latitude, mean longitude) of two points (*G*, *L*), where *G* is the geographic mean of the epicenters of the decelerating preshocks and *L* is the geographic mean of the previous known mainshocks located in the corresponding seismogenic region (see section 2.3).

We consider as predicted origin time, t_c^*, and magnitude, M^*, the corresponding average values estimated by the two models and as predicted epicenter, $E^*(\phi,\lambda)$, the geographic mean (mean latitude, mean longitude) estimated by the two models. The 2σ uncertainties of these estimated (predicted) values by both models are:

$$\Delta t_c \leq 5.0 \text{ years}, \qquad \Delta M \leq 0.4, \qquad \Delta x \leq 200 \text{ km}. \tag{14}$$

4. Backward tests of the two models

The TIMAPR and D-AS time-dependent seismicity models have been extensively examined during the last decade, leading to the identification of several predictive and physical properties of both models. In this section we use recent global data which are reliable and have not been used in the development of these models (Papazachos *et al*., 1997, 2006b), aiming at testing the validity of their properties. The data used concern the last two strong mainshocks (*M*=6.3-9.0) of each one of the ten large areas of the continental fracture system considered in the present work. The origin times, t_c, the epicenter coordinates, $E(\phi,\lambda)$, and moment magnitudes, *M*, of these twenty mainshocks are listed in Table 1. This is an appropriate data sample because it

encompasses mainshocks that occurred in various tectonic settings and in a broad magnitude range, including the three great (M~9) earthquakes of the past decade (Sumatra 2004, South America 2010, Japan 2011).

4.1. Backward tests of the TIMAPR model

This model is applied on a declustered catalogue of mainshocks resulted from the procedure described in section (2.2), adopting a declustering time window equal to 15 years. The interevent times of these mainshocks have quasi-periodic properties and, along with their magnitudes, follow Eqs. (1), (2), (3) and (4) which are used to predict the origin time, t_t, and the magnitude, M_t, of an ensuing mainshock. For this reason, two backward tests have to be performed to the data related to the twenty mainshocks in order to test the validity of these two basic model properties, namely the length of the declustering time window and the retrospective estimation (prediction) of the twenty mainshocks.

The available instrumental (1900-2011) complete data of earthquakes that occurred in each one of the seismogenic regions (defined in section 4.2) of the mainshocks listed in Table 1 were used to test the validity of the adoption of Δt=15 years as the optimum value of the declustering time window for obtaining a ratio σ/T <0.50, which holds for a declustered mainshock catalogue with quasi-periodic behavior. Fig. 2 shows the variation of the mean value of this ratio against Δt (thick black line), calculated for each seismogenic region for Δt values between 1 and 25 years. The dashed lines correspond to one standard deviation. It is observed that for Δt>15 years all three curves denote ratio values smaller than 0.5. For this reason we may reasonably conclude that this time window is appropriate for declustering the original (complete) catalogue of a seismogenic region in order to compile a catalogue of mainshocks with quasi-periodic properties.

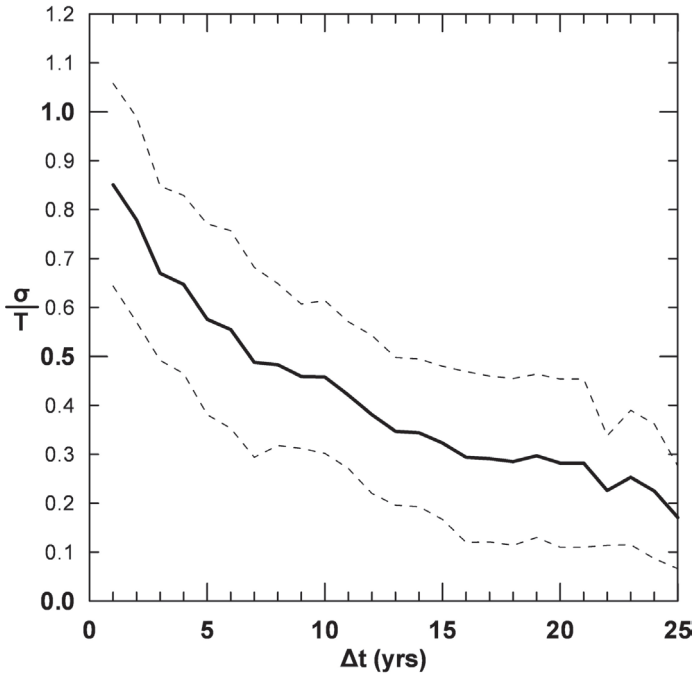

Fig. 2 - Variation with the declustering time window, Δt, of the average value, σ/T, of the twenty such ratios calculated for each time step and each of the twenty seismogenic regions of the mainshocks listed in Table 1 (thick line). Dashed lines show the variation of one standard deviation of this quantity. For Δt>15 years, all three lines show ratio values smaller than 0.5 and almost constant.

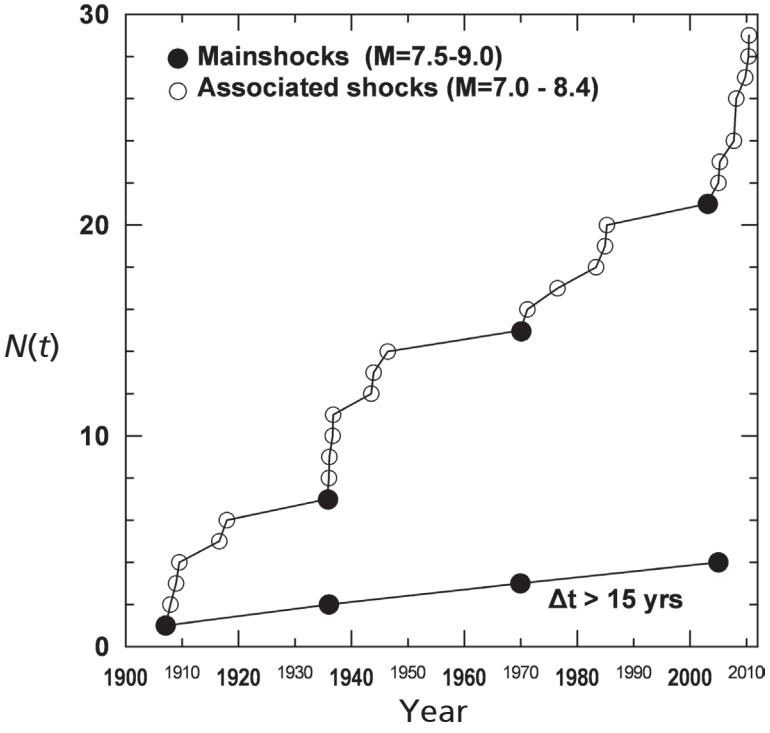

Fig. 3 - Time variation of the cumulative number, $N(t)$, of shocks in the seismogenic region of the Sumatra 2004 great earthquake (M=9.0), for the complete (upper part) and the declustered (lower part) catalogue, respectively. Mainshocks are denoted by black circles (M=7.5-9.0) and associated shocks (aftershocks etc.) by open circles (M=7.0-8.4).

To further check the declustering procedure followed we plotted the cumulative number of shocks of the complete (clustered) earthquake catalogue of each region against time. We found that for each one of the catalogues of the regions examined, the number of groups (clusters in time) is equal to the number of mainshocks defined by the applied declustering procedure, and that the largest earthquake of each cluster is the corresponding large mainshock of the residual (declustered) catalogue of the region. Fig. 3 shows an example of the application of the declustering procedure on the earthquake catalogue of the seismogenic region of the Sumatra 2004 earthquake.

As regards predictions with the TIMAPR model we applied the procedure described in section (2.2) in each one of the twenty seismogenic regions (with center F, and radius a, see Table 2) to compile the mainshock catalogues which were subsequently used to calculate [by Eqs. (1), (2), (3) and (4)] the retrospectively predicted, by this model, origin time t_t, and magnitude M_t for each one of the twenty strong recent earthquakes listed in Table 1.

4.2. Backward tests of the D-AS model

To examine the basic properties of the D-AS model that may be of predictive and/or physical significance, we carried out the following tests: a) we checked whether each mainshock from those listed in Table 1 had been preceded by a decelerating and an accelerating seismic sequence, both easily identifiable and well defined in space and time, consisting of shocks larger than certain cut-off magnitudes, different for each sequence, b) we also checked the relation between the start times of the two preshock sequences as well as the frequency-magnitude distribution of the shocks of these sequences, which may contribute to the explanation of the physical process that culminates in the mainshock generation, and c) we attempted retrospective predictions for the twenty mainshocks.

a) After a grid search (grid 5°×5° around the mainshock epicenter with spacing 0.5°) we found two distinct geographical points where the strain deceleration index, q_{df}, and the corresponding strain acceleration index, q_{aq}, have their largest values. These points correspond to the center F, of the circular seismogenic region with radius a [given by Eq. (10)] and to the center Q, of circular critical region with radius R [given by Eq. (7)]. Information on F, Q, a, and R is given in Table 2, along with the values of q_{df} and q_{aq}. We also determined the indexes q_{de} and q_{ae} from shocks located in circular regions (with radii a and R, respectively) centered at the mainshock epicenter. It is observed that strain deceleration in the seismogenic region and strain acceleration in the critical region have large values, in agreement with those calculated from global data (see section 3.1), in contrast to the small values of these indexes determined in the circular regions around the mainshock epicenter, which in turn agrees with the observations of Hardebeck *et al.* (2008). An example of the spatial distribution of the decelerating (dots) and accelerating (small open circles) preshocks of the Sumatra, 2004 mainshock is shown in Fig. 4. Plots of the time variation of the decelerating and accelerating Benioff strain release, *S(t)*, are also shown at the lower part of the figure, along with the curves that fit the data. It is noted that both sequences end when the largest values of q_{df} and q_{aq} have been calculated (see section 3.1).

b) In all accelerating preshock sequences examined the start year is, on average, about 8 years smaller than the start year of the corresponding decelerating sequence. This verifies the early start of the accelerating seismic sequence in respect to the decelerating sequence of a

Table 2 - The geographic centers, $F(\phi,\lambda)$, $Q(\phi,\lambda)$, and the corresponding radii, a (in km), R (in km), of the seismogenic and critical region, respectively, of the two last mainshocks of each of the ten areas of the continental fracture system. The q_{df} and q_{aq} are the strain deceleration and the strain acceleration in the circular seismogenic (F, a) and in the circular critical (Q, R) region, respectively. The q_{de} is the strain deceleration and the q_{ae} is the strain acceleration in the corresponding circular regions centered on the mainshock epicenter, E.

Area	$F(\phi,\lambda)$	a(km)	$Q(\phi,\lambda)$	R(km)	q_{df}	q_{de}	q_{aq}	q_{ae}
W. Mediterranean	34.7, 04.1 37.0, -05.7	227 175	35.7, 05.3 35.5, -06.0	346 292	10.6 8.1	3.1 1.7	3.7 3.8	1.3 0.5
Aegean	36.0, 20.9 35.9, 25.8	137 139	34.6, 23.7 35.2, 29.5	420 113	6.8 11.4	4.1 0.5	4.6 6.8	2.0 0.4
Cyprus	36.2, 31.6 38.5, 34.3	139 195	36.5, 27.5 35.6, 35.5	248 199	7.8 5.5	2.9 0.6	9.0 10.7	1.9 2.7
Anatolia	41.8, 27.6 38.7, 44.0	244 207	36.9, 28.0 37.9, 40.0	321 423	9.1 8.9	4.0 1.6	8.7 12.6	3.4 2.9
Central Asia	35.0, 81.5 29.0, 62.2	81 156	37.0, 78.7 29.7, 61.1	423 469	5.3 9.9	0.3 0.5	5.0 5.2	3.0 0.2
Sumatra	-11.2, 113.5 02.4, 97.6	211 631	-15.0, 111.2 01.9, 95.9	682 2484	10.5 7.1	1.9 6.4	6.1 11.4	2.1 8.5
Japan	42.1, 141.7 37.3, 141.2	188 364	41.4, 143.6 36.8, 138.4	1590 1815	7.7 5.3	5.1 3.7	4.4 5.5	4.4 5.4
N. Pacific	52.0, 179.9 45.7, 154.5	143 325	55.6, 179.3 50.9, 156.9	542 751	5.6 10.5	4.9 8.5	5.7 5.4	4.0 2.8
California	40.1, -122.8 32.1, -117.4	131 202	36.6, -120.6 29.1, -112.7	261 406	6.0 7.4	2.9 3.8	5.5 4.9	0.4 0.7
S. America	-18.5, -74.9 -36.9, -74.9	252 533	-12.5, -73.6 -34.0, -75.7	838 2002	12.8 11.7	1.9 4.6	8.6 3.6	4.9 1.2

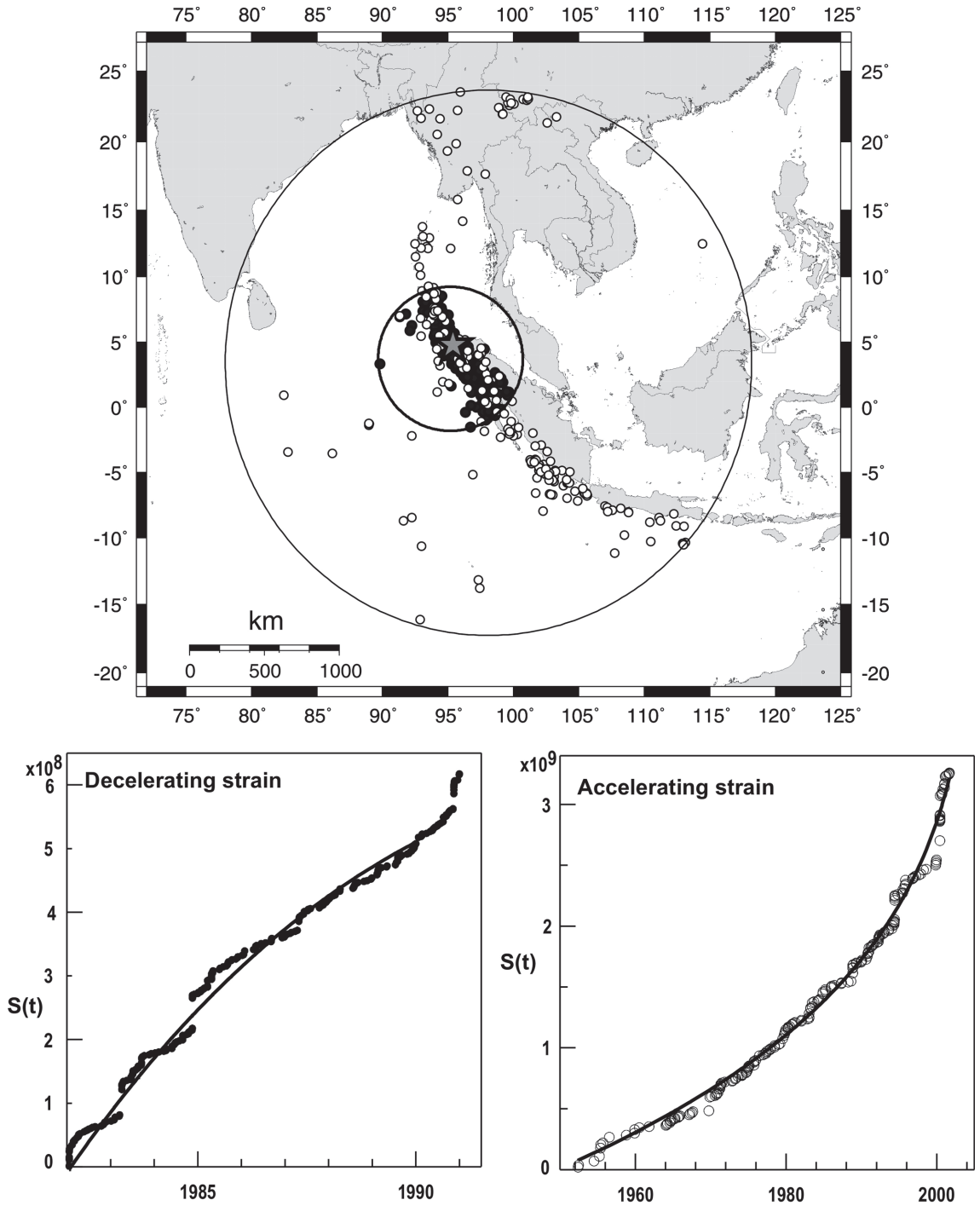

Fig. 4 - Information on the decelerating-accelerating seismicity which preceded the Sumatra great earthquake (26.12.2004, M=9.0). Dots (in the upper part) are epicenters of decelerating preshocks which are included in the circular seismogenic region, small open circles show epicenters of accelerating preshocks located in the circular critical region and the star shows the mainshock epicenter. The time variation of the decelerating and accelerating Benioff strain, $S(t)$, is shown in the lower part of the figure. The best fit curves of the time variation of the Benioff strain, which follow the power-law Eq. (5), are also shown.

mainshock found in previous work (e.g. Papazachos *et al*., 2006b; Karakaisis *et al*., 2013). In all accelerating preshock sequences the largest preshocks occurred in the second half of their duration. This increase of magnitude (decrease of *b* value) in the second half of the accelerating preshock sequence supports the critical triggering by accelerating preshocks since it corresponds to the commencement of the decelerating preshock sequence (its excitational phase) in the seismogenic region, i.e. accelerating preshocks trigger (by stress transfer in a quasi-static mode) strong decelerating preshocks which further trigger the mainshock (by stress transfer in static mode) because they have their foci in the vicinity of the mainshock focus. Triggering of very high seismic activity in the seismogenic region is probably due to the clustering of very active seismic faults (network of faults) in this region. The excitation in the beginning of the decelerating sequence results in the subsequent seismic quiescence and the creation of the decelerating pattern in the seismogenic region. This is because most of the large faults in this region break during the first phase and few unbroken faults are left to be ruptured during the second (quiet) phase. Among the unbroken faults is the fault of the mainshock which breaks later because it requires strong triggering, caused by the quasi-static triggering of the far located accelerating strong preshocks and by the static triggering caused by strong decelerating preshocks that occur close to the mainshock epicenter during the first (excitational) phase of the decelerating sequence.

c) The predictive properties of the D-AS model are tested through the retrospective prediction of the origin times, t_d, and magnitudes, M_d, of the twenty mainshocks of Table 1, which are listed in the same table. It is observed that these values are within the corresponding error windows given by Eqs (14).

The finally adopted origin times, t_c^*, and magnitudes, M^*, are the mean values that have been calculated by the two models and are also listed in Table 1. In this table the retrospectively predicted (by both models) epicenter coordinates, $E^*(\phi,\lambda)$, of each mainshock (mean value of the geographical points *G* and *L*) are also listed. The distance, *EE**, between the predicted and the observed epicenters for all twenty cases is also within the error window given by the last of Eq. (14).

We can conclude here that tests of the two models on a representative sample of recent global observations verify the known basic predictive and physical properties of both models and that the results of these tests strongly support the notion that the combined application of these models may constitute a promising method for intermediate-term prediction of strong mainshocks.

4.3. Probabilities for random occurrence of the retrospectively predicted mainshocks

Calculation of the probability for random occurrence of a mainshock within the predicted space, time and magnitude windows is necessary because if this probability is comparable to that one calculated by the D-AS model (~80%), then the corresponding prediction is practically meaningless. Calculation of probability for random occurrence is usually based on the assumption that the magnitudes of the earthquakes of the sample used are distributed according to the G-R recurrence law (Gutenberg and Richter, 1944) and their times follow a simple Poisson distribution.

We determined the frequency-magnitude distribution of complete samples of earthquakes with $M \geq 5.2$ and $h \leq 100$ km that occurred during 1964-2011 in each one of the predicted circular

regions with center, E^*, and r=200 km, by applying the well known G-R relation:

$$\log N_t = a_t - bM \tag{15}$$

After reducing the constant a_t to each annual value, a, we calculated the probability, $P_r(M)$, for random occurrence of an earthquake with magnitude M or larger during the prediction time window t (=10 years) by the relation:

$$P_r = 1 - \exp\left(-\frac{t}{T}\right) \tag{16}$$

where $T=10^{bM-a}$ and t=10 years (the prediction time window). Since the predicted magnitude window by the D-AS model is $M\pm0.4$, the difference in the probabilities obtained by Eq. (16) for the two magnitude limits, allows assessing the probability for random occurrence of the earthquake in the predicted magnitude window.

The calculated probabilities for random occurrence, $P_r(M)$, of each one of the probably ensuing mainshocks are listed in Table 3. It is observed that most (~75%) of the probability values are smaller than 20%, meaning that there is a low ratio of random/D-AS probabilities. However, one may argue that the test for random occurrence described above is too simple and more sophisticated tests are needed to check the validity of the D-AS model. Results of such tests have been published elsewhere but such test is also performed in the present section.

The first test is based on the application of the grid search method on synthetic random catalogues, following the procedure suggested by Zöller *et al*. (2001). It was found (Papazachos *et al*., 2006b) that the probability for random occurrence of decelerating Benioff strain only is 0.10 and the probability for random occurrence of accelerating strain only is 0.30. Therefore, the probability for simultaneous random occurrence of both patterns is very low.

The second test is based on comparison of the results of the D-AS model with the results of the G-R model by the so called R-test (Martin, 1971). It has been shown that the results of the D-AS model and of the G-R model are clearly distinguishable (Papazachos *et al*., 2007b, 2009). Consequently, the performance of the model can be objectively tested after expiration of the end of the prediction times of all predicted mainshocks in an area.

The third method has recently been proposed by Harderbeck *et al*. (2008) and concerns tests of observed accelerating seismicity against synthetic catalogs that include spatiotemporal clustering. Such tests applied for the Aegean area and for California (Karakaisis *et al*., 2013) have shown that observed precursory accelerating seismicity in the broad (critical) region and observed decelerating seismicity in the narrow (seismogenic) region are both statistically significant to a very high significance level, for mainshocks in the magnitude range 6.4-7.1.

We present an example of the latter test for the areas of Japan, California and Aegean, following the procedures suggested by Zöller *et al*. (2001) and Hardebeck *et al*. (2008). We examined these areas because of their high seismicity and because of the wide magnitude range of the mainshocks examined (6.4-9.0). We used a complete sample of six large ($M\geq7.5$) shallow mainshocks that occurred in the broader area of Japan after 1980 (1983 M=7.7, 1993 M=7.5, 1994 M=8.3, 1994 M=7.7, 2003 M=8.3, 2011 M=9.0) and two complete samples of eight strong (M=6.4-7.1) shallow mainshocks that occurred in California and the Aegean after 1995

Table 3 - Information on the results of the forward tests of the two models, concerning 29 circular seismogenic regions located in ten areas of the continental fracture system. The names of these areas and their geographic boundaries are given in the first two columns of the table. M_{mp} is the minimum magnitude of the predictable mainshocks in each of these areas. The t_c^*, M^* and $E^*(\phi,\lambda)$ are the estimated (predicted) origin times, moment magnitudes and epicenter coordinates (by both models) of the probably ensuing mainshocks. The uncertainties of these estimated values are: ≤5.0 years for the origin time, ≤0.4 for the magnitude, and ≤200 km for the epicenter of the mainshock, with probability 80%. The probabilities, $P_r(M)$, for random occurrence are also shown.

Area	Geographic boundaries	M_{mp}	n	t_c^*	M^*	$E^*(\phi,\lambda)$	$P_r(M)$
W. Mediterranean	35.0N - 47.0N 11.0W - 19.0E	7.0	1	2016.3	7.6	37.3N, 10.0W	0.11
			2	2014.7	7.2	43.1N, 00.5W	0.02
			3	2017.0	7.1	44.8N, 16.9E	0.01
			4	2018.7	7.2	40.8N, 15.5E	0.12
Aegean	34.0N - 41.0N 19.0E - 28.0E	6.5	5	2015.8	6.7	39.5N, 20.4E	0.54
			6	2013.7	7.1	38.1N, 20.8E	0.41
			7	2013.3	7.2	39.9N, 24.8E	0.33
			8	2015.2	7.3	35.4N, 25.4E	0.09
Cyprus	34.0N – 37.0N 32.0E – 36.0E	6.5	9	2014.5	6.8	36.4N, 34.4E	0.24
Anatolia	37.0N - 42.0N 28.0E - 44.0E	7.0	10	2018.2	7.6	40.0N, 28.8E	0.21
			11	2016.6	7.3	40.5N, 40.1E	0.23
Central Asia	20.0N - 44.0N 64.0E - 90.0E	7.5	12	2017.0	7.8	42.1N, 68.8E	0.01
			13	2016.8	7.8	24.6N, 67.6E	0.02
			14	2015.5	7.5	41.2N, 86.7E	0.09
			15	2015.0	7.5	33.3N, 79.4E	0.06
Sumatra-Java	12.0S - 10.0N 90.0E - 120.0E	8.5	16	2016.2	8.8	09.9S, 108.1E	0.01
Japan	30.0N - 46.0N 128.0E – 148.0E	7.5	17	2016.1	7.8	32.9N, 132.5E	0.17
			18	2014.9	7.5	34.8N, 134.8E	0.09
			19	2015.8	7.5	38.5N, 139.8E	0.36
N. Pacific	45.0N - 65.0N 150.0E – 140.0W	8.5	20	2015.7	9.0	46.2N, 151.5E	0.02
			21	2015.2	8.6	51.5N, 178.6E	0.14
			22	2013.7	8.8	53.3N, 163.9W	0.02
			23	2015.1	8.7	62.2N, 146.0W	0.12
California	33.0N - 39.0N 115.0W - 123.0W	7.5	24	2016.6	7.7	36.2N, 120.0W	0.05
			25	2014.3	7.9	37.4N, 117.5W	0.01
S. America	35.0S - 05.0N 65.0W - 85.0W	8.0	26	2016.6	8.6	29.9S, 73.3W	0.02
			27	2014.4	8.1	13.8S, 72.5W	0.01
			28	2015.2	8.7	06.2S, 76.0W	0.03
			29	2016.7	8.7	04.0N, 77.8W	0.02

(California: 2010 M=6.5, 2010 M=7.1, Aegean: 1995 M=6.6, 1995 M=6.4, 2001 M=6.4, 2006 M=6.9, 2008 M=6.7, 2009 M=6.4).

The earthquake catalogue of Japan was initially declustered. The spatial window, where aftershocks following a mainshock with magnitude M occur, was defined as a circular region

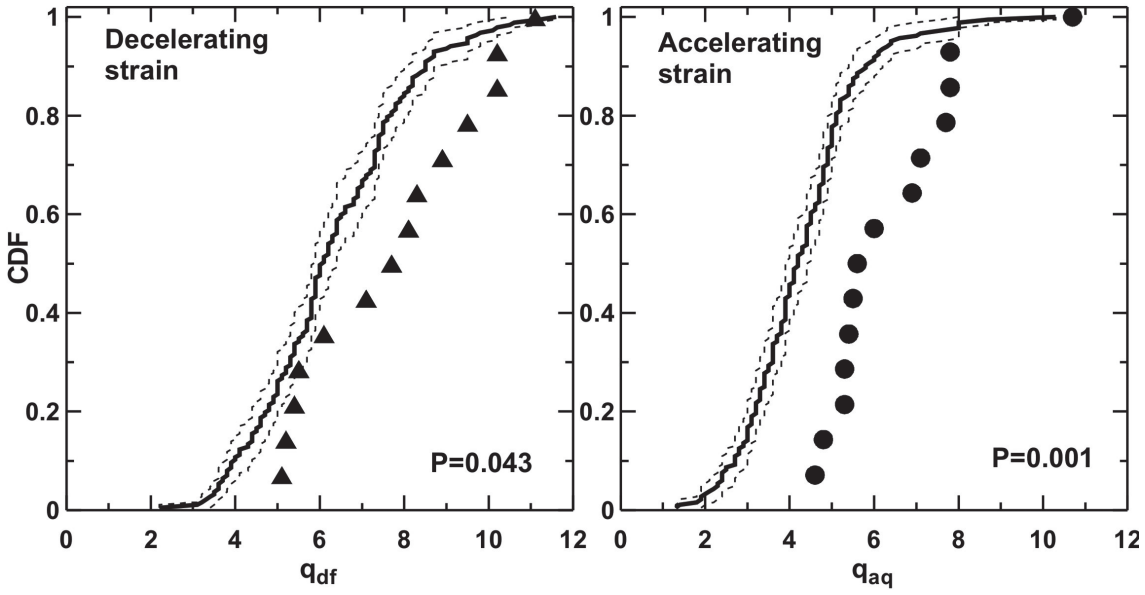

Fig. 5 - Cumulative distribution function (CDF) of the strain deceleration, q_{df} (triangles, left graph) in the seismogenic regions and the strain acceleration, q_{aq} (dots, right graph) in the critical regions of all fourteen mainshocks (M=6.4-9.0) that occurred in Japan after 1980 and in California and the Aegean after 1995 (see text for explanation). Continuous lines show the CDF curves of the strain deceleration (left graph part) and strain acceleration (right graph) which preceded the mainshocks of synthetic catalogues with spatio-temporal clustering generated for these three regions, while the corresponding dashed lines show the 95% confidence intervals determined by bootstrap resampling. Small values of probability, P, of a Kolmogorov-Smirnov test show that the CDF of the real data, concerning q-values calculated for the fourteen mainshocks, is significantly different from that of the data of the synthetic catalogues.

centered on the mainshock epicenter with radius L(km)=0.02 $\times 10^{0.5 \cdot M}$, derived by Kagan (2002) whereas the temporal window is based on the relation log$T$(yrs)=-3.5+0.5·M (Utsu, 1969). The resulted declustered catalogue was used to determine the spatially varying background seismicity rate in each of the 1×1° cells over the examined area and considering a Poisson time distribution of the origin times and the G-R distribution for the magnitudes (with b=1), we estimated the corresponding random spatio-temporal earthquake distributions. We then added aftershocks which decayed according to the modified Omori's law (Utsu, 1961) with $\overline{p}$ =1.08 (Nanjo *et al.*, 1998). Ten synthetic catalogues were thus compiled for Japan and the D-AS model was applied to all M≥7.5 shocks that occurred after 1980 in each catalogue. The above described procedure was applied to the data of California and Aegean and twenty synthetic catalogues were also created (10 for California and 10 for the Aegean) and all shocks with M≥6.4 after 1995 were examined (details on the parameters used for the compilation of the latter synthetic catalogues with spatio-temporal clustering can be found in Karakaisis *et al.*, 2013). After the grid search procedure described previously we identified the geographical points where the maximum decelerating and accelerating strain, q_{df} and q_{aq}, respectively, are observed.

Fig. 5 shows the cumulative distribution of the strain deceleration (triangles, in the left part of the figure) in the fourteen circular seismogenic regions and the strain acceleration (dots, in the right part of the figure) in the respective circular critical regions for the mainshocks examined. The continuous lines in this figure show the cumulative distribution function of the same indexes of the synthetic catalogues with spatio-temporal clustering, and the dashed lines

show the 95% confidence intervals based on bootstrap resampling (1000 samples of the q_{df} and q_{aq} values of the synthetic data were generated). Such confidence intervals were also defined for the observed values of strain deceleration and strain acceleration and were also used in determining the probabilities for random occurrence of the decelerating precursory seismicity in the seismogenic regions and of the accelerating precursory seismicity in the critical regions of these strong mainshocks in Japan, California and the Aegean. The result is that the probability, estimated through a two-sample Kolmogorov-Smirnov test (Press *et al.*, 1986), that q values of real and synthetic catalogues have been drawn from the same population, is very low (P=0.043 for decelerating strain and P=0.001 for accelerating strain). Consequently, the probability for random occurrence of both patterns before a mainshock (as the D-AS model requires) is negligible.

Therefore, the result of the applications of these three methods is that relative observations against synthetic catalogues support the non-random occurrence of precursory decelerating seismicity in the narrow (seismogenic) region and of the accompanying accelerating seismicity in the broader (critical) region, in accordance with the D-AS model.

5. Forward tests of both models

Although the tests performed on the two time-dependent seismicity models, and particularly on the D-AS model, showed that they may adequately represent the time variation of past seismicity, prediction of future strong earthquakes is needed to check objectively the merits and handicaps of these and other similar models.

Such forward tests have been already made for the D-AS model and led to interesting conclusions which were taken into consideration in the revised version of the model applied in the present work. One of the important such conclusions is the generation of the mainshocks systematically later than the initially predicted time window. For this reason, this precursory seismic pattern has been monitored systematically in the Aegean area by repeating every year the calculations required by the D-AS model. This procedure led to a preliminary false alarm for the Cythera strong earthquake (8 January 2006, M=6.9, ϕ=36.2°N, λ=23.4°E) when data up to the end of 2000 were used. However, the same procedure led to the final successful prediction (t_c^*=2006.1, M^*=6.9, ϕ^*=36.5°N, λ^*=22.7°E) when data up to the end of 2002 were used (Papazachos *et al.*, 2007a). This problem is tackled in the present work by using improved relations for predictions based on the D-AS model and by performing independent estimations (predictions) by the TIMAPR model.

Another interesting result of this systematic monitoring of seismicity in the Aegean area is the successful prediction by the D-AS model (Papazachos *et al.*, 2009) of the strong (M=6.4) earthquake which occurred on 17 July 2008 in eastern Aegean (ϕ=36.0°N, λ=27.9°E) and caused damage in Rhodos island.

It takes much time (some years) to verify or not the result of forward tests for such time dependent models. For this reason, such tests must be carefully organized by taking into consideration results of backward tests (see section 4.2), results of tests on synthetic catalogues (see section 4.3) and results of previous forward tests (Papazachos *et al.*, 2006a, 2007a, 2007b, 2009, 2010b). These results, in addition to their importance for improving the predictive

relations of the two models, indicated certain constrains (limitations) which must be taken into account when a forward test is scheduled. Such important constrains are the accurate definition of the geographical boundaries of the area where the forward tests are applied (e.g. of Japan, Aegean, California, etc) and the estimation of the minimum magnitude of the mainshocks which are predictable by both models. The magnitude M_{mp} of the smallest predictable mainshock for each of the ten areas for which both models indicate oncoming mainshocks is given in Table 3 along with the geographic boundaries of these ten areas.

The smallest predictable mainshock by the two models in each of the ten areas depends on the long-term seismicity level of the area and particularly on the magnitude of the largest earthquake occurred in the area. Thus, most of the earthquakes in the magnitude range 6.3-7.0 are associated shocks (aftershocks, foreshocks, preshocks, postshocks) in Japan (where the magnitude of the largest instrumentally recorded earthquake is 9.0), while most shocks of this magnitude range are mainshocks in Mediterranean (where the magnitude of the largest instrumentally recorded earthquake is 7.5). Furthermore, the smallest predictable mainshock by the D-AS model in an area and during a time interval depends also on the maximum spatial extend of the already occurring preshock and aftershock activity in the area during the prediction time window. Thus, the magnitude of the smallest predictable earthquake by the D-AS model in an area during a certain time period depends on the magnitude of the largest expected main shock in the area, because if this magnitude is large, a considerable part of the area is covered by epicenters of preshocks of the largest ensuing mainshock and preshocks of smaller oncoming mainshocks cannot be distinguished.

Taking these constrains into consideration, the algorithm concerning the D-AS model was applied to identify in each of the ten areas pairs of decelerating–accelerating seismic sequences and corresponding pairs of seismogenic–critical regions and to attempt estimation (prediction) by this model probably ensuing strong (6.3-9.0) mainshocks. Information on the seismogenic regions defined in this way for each of the ten areas are used to apply the TIMAPR model for predicting by this model also probably ensuing strong (6.3-9.0) mainshocks. Table 3 gives the results of these forward tests. The t_c^*, M^* are the joint (and finally adopted) results of the two models (mean values of the calculated ones by both models). $E^*(\phi,\lambda)$ are the expected mainshock epicenter coordinates based on both models. The corresponding uncertainties Δt_c, ΔM, Δx are given by Eq. (14). The probability for random occurrence, $P_r(M)$, of these mainshocks is also shown.

The number of the estimated (predicted) events for each of the ten areas of the continental fracture system was compared with the number resulted from the observed rate of corresponding mainshocks which occurred in the same area during the instrumental period, in order to check whether these estimations are realistic. It is found that, for the nine of the ten areas, the number of the estimated (predicted) events is compatible with the number resulted from the observed rates (see an example in Fig. 6 concerning North Pacific). The discrepancy between estimated number and observed rate concerns West Mediterranean where the estimated (predicted) number of strong ($M \geq 7.0$) events during the next decade (2013-2022) is four, while the total number of earthquakes with $M \geq 7.0$ that occurred in this area during the instrumental period (1900 -2011) is only five, and none of these instrumentally recorded strong earthquakes is located in any of the seismogenic regions of West Mediterranean defined in the present work by the two models. On the contrary, historical (1500 -1800) strong earthquakes are located in every one of these

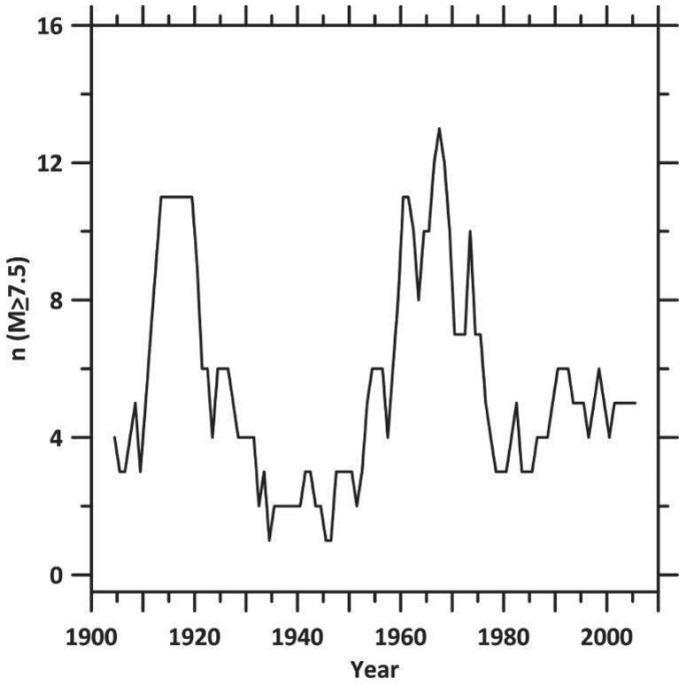

Fig. 6 - Time variation of the frequency (number of events per decade) of the large (M≥7.5) earthquakes that occurred in the whole active area of North Pacific during the instrumental period. The pattern indicates that the low frequency observed since 1980 may be followed by the start of a seismic excitation during the next decade.

four estimated regions. This last observation suggests that the four seismogenic regions of West Mediterranean defined in the present work must be considered as candidate for the generation of strong mainshocks as long as this is indicated by the application of the two models on reliable (new) data.

Due to successful testing of these two time dependent models by techniques (backward tests, tests on synthetic catalogues) of which the results are already known, and to the large sample of reliable global data on which forward tests are based, we may expect that these forward tests to have important positive implication on the knowledge of time dependent seismicity as well as of time dependent seismic hazard (e.g. by considering currently active seismogenic regions as seismic zones for time dependent seismic hazard assessment). That is, positive results of these forward tests may lead to significant implications of social interest.

6. Conclusions and discussion

Backward tests were performed for the TIMAPR model, based on interevent times of twenty recent (1994-2011) strong (M=6.3-9.0) mainshocks occurred in the continental fracture system (Mediterranean-Indonesian and circum-Pacific seismic zones). Corresponding tests for the D-AS model, based on triggering of the twenty mainshocks by their preshocks, were also performed. The results of these backward tests support the following conclusions:

Each strong shallow (h≤100 km) mainshock is preceded by a decelerating and an accelerating preshock sequence. Both sequences are easily identifiable in space, time and magnitude windows before the generation of their mainshock. These windows are different for decelerating and accelerating preshocks of a mainshock.

Preshocks trigger the generation of their mainshock and their space, time and magnitude distributions allow its intermediate-term prediction. Comparison of the observed parameters for the twenty recently occurred mainshocks with their retrospectively predicted parameters allowed estimation of the uncertainties, which are within the error windows of the models.

The circular seismogenic region of a mainshock is accurately defined by the epicenters of decelerating preshocks. This region includes a system (network) of very active seismic faults where large earthquakes are clustered. These mainshocks have a quasi-periodic behavior. That is, the mainshocks in a seismogenic region (which behave as the characteristic earthquakes in a seismic fault) are easily detected by the available seismic observations (instrumental, historic). Thus, interevent times of the mainshocks located in a seismogenic region follow the TIMAPR model and allow the intermediate-term prediction of an ensuing mainshock in the region by this model too.

Although the curvature parameter, *C*, has been widely used for optimization of accelerating seismicity, it has been shown (Mignan, 2008, 2011) that this optimization procedure is simplistic and may lead to unstable and erroneous results. Moreover, most of the relevant published research work concerns search of accelerating seismicity around the epicenter of an occurred (or ensuing) mainshock, but such precursory accelerating seismicity is statistically insignificant (Hardebeck *et al*., 2008), since its level is very low (Karakaisis *et al*., 2013).

The D-AS model we apply is different from the approach mentioned above because: a) this model considers precursory decelerating and accelerating seismicity not around the epicenter of an ensuing mainshock but in the well-defined seismogenic and critical regions, respectively. These two precursory patterns (decelerating, accelerating) of an ensuing mainshock occur also in different time and magnitude windows. The centering of the precursory accelerating seismicity away from the epicenter of the ensuing mainshock is also supported by work on critical regions of New Zealand and China (Yang *et al*., 2001). b) The optimization parameters q_{df} and q_{aq} [Eqs. (6) and (9)] take into consideration the curvature, *C*, but also the parameter, *m*, of Eq. (5) as well as the probabilities (P_a, P_d) for satisfying the global Eqs. (7), (8), (10) and (11) which have been derived by large samples of precursory seismic sequences. c) Statistical tests on relative reliable observations against synthetic catalogues with spatio-temporal clustering published (Karakaisis *et al*., 2013) or performed in the present work (Fig. 5) verify precursory decelerating and accelerating seismicity expected by the D-AS model. d) Forward tests of this model in the Aegean area (where relative monitoring is systematic) led to the successful prediction of the last strong mainshock in the western part of the Hellenic Arc (Papazachos *et al*., 2007a) and of the last strong mainshock in the eastern part of this arc (Papazachos *et al*., 2009).

Forward tests of the two time dependent seismicity models resulted in the identification of currently active pairs of decelerating-accelerating seismicity patterns and corresponding seismogenic regions in each of the predefined ten areas. Inter-event times of the mainshocks located in each identified seismogenic region and properties of decelerating and accelerating preshocks led to the estimation (prediction) of the parameters of probably ensuing strong shallow events in each of the ten large areas of the continental fracture system.

The number of estimated (predicted) strong events in each one of the nine areas (Aegean, Cyprus, Anatolia, Central Asia, Sumatra-Java, Japan, North Pacific, California, South America) of the continental fracture system is compatible with the mean rate of the mainshocks with the same minimum magnitude generated in the corresponding area during the instrumental period

(1900 -2011). This, however, does not hold for West Mediterranean where the number of the estimated strong events for the next decade is much larger than the number resulted from the rate of corresponding mainshocks generated during the instrumental period.

Discrepancies between predictions made by this method, and corresponding observations, like the one concerning West Mediterranean, can be understood if three possible results of these forward tests are taken into consideration. The first possibility is that the predicted event by the method is a mainshock. A second possibility is that the predicted event corresponds to a strong associated shock (preshock) or to a barrier which will break during the rupture of the mainshock fault when the largest barrier of the fault will also break. A third possibility is a false alarm which can be preliminary, that is, the predicted mainshock to occur out (later) of the predefined time window. These possibilities are part of the goal of these forward tests, that is, of the objective determination of the predictive ability of this method, which means objective determination of successful predictions, false alarms and failures.

It must be finally pointed out that the goal of the present work is to improve knowledge on time-dependent seismicity. For this reason the present paper is addressed to relative scientists only.

Acknowledgements. We are grateful to the two anonymous reviewers and the Associate Editor (Lawrence Hutchings) for their constructive criticism that helped to improve our work and clarify certain aspects. Thanks are due to Wessel and Smith (1995) for freely distributing the GMT software used to produce the maps of the present article. This work was supported by the THALES Program of the Ministry of Education of Greece and the European Union in the framework of the project entitled "Integrated understanding of Seismicity, using innovative Methodologies of Fracture mechanics along with Earthquake and non-extensive statistical physics – Application to the geodynamic system of the Hellenic Arc. SEISMO FEAR HELLARC".

REFERENCES

Ben-Zion Y. and Lyakhovsky V.; 2002: *Accelerated seismic release and related aspects of seismicity patterns on earthquake faults*. Pure Appl. Geoph., **159**, 2385-2412.

Bowman D.D., Quillon G., Sammis C.G., Sornette A. and Sornette D.; 1998: *An observational test of the critical earthquake concept*. J. Geophys. Res., **103**, 24359-24372.

Brehm D.J. and Braile L.W.; 1999: *Intermediate-term earthquake prediction using the modified time-to-failure method in southern California*. Bull. Seism. Soc. Am., **89**, 275-293.

Bufe C.G. and Varnes D.J.; 1993: *Predictive modeling of seismic cycle of the Great San Francisco Bay Region*. J. Geophys. Res., **98**, 9871-9883.

Engdahl E.R. and Villaseñor A.; 2002: *Global Seismicity: 1900-1999*. In: Lee W.H.K., Kanamori H., Jennings P.C. and Kisslinger C. (eds), International Handbook of Earthquake and Engineering Seismology, Part A, chapter 41, Academic Press, pp. 665-690.

GCMT (Global Centroid Moment Tensor Catalogue Search); 2012: http://www.globalcmt.org/CMTsearch.html.

Gomberg J., Beeler N.M., Blanpied M. L. and Bodin P.; 1998: *Earthquake triggering by transient and static deformations*. J. Geophys. Res., **103**, 24411-24426.

Gutenberg B. and Richter C.F.; 1944: *Frequency of earthquakes in California*. Bull. Seism. Soc. Am., **34**, 185-188.

Helmstetter A.; 2003: *Is earthquake triggering driven by small earthquakes?* Physical Review Letters, **91**, 58501-58504.

Hardebeck J.L., Felzer K.R. and Michael A.J.; 2008 : *Improved tests reveal that the accelerating moment release hypothesis is statistically insignifiant*. J. Geophys. Res., **113**, 808310, doi:10.1029/2007JB005410.

ISC (International Seismological Centre); 2012: ***On-line Bulletin***. http://www.isc.ac.uk/Bull, Internat. Seis. Cent., Thatcham, United Kingdom.

Kagan Y.Y.; 2002: *Aftershock zone scaling*. Bull. Seismol. Soc. Am., **92**, 641–655.

Kagan Y.Y. and Jackson D.D.; 1991: *Long-term earthquake clustering*. Geophys. J. Int., **104**, 117-133.

Karakaisis G.F., Papazachos C.B., Panagiotopoulos D.G., Scordilis E.M. and Papazachos B.C.; 2007: *Space distribution of preshocks*. Boll. Geof. Teor. Appl., **48**, 371-383.

Karakaisis G.F., Papazachos C.B., and Scordilis E.M.; 2013: *Recent reliable observations and improved tests on synthetic catalogs with spatiotemporal clustering verify precursory decelerating-accelerating seismicity.* J. Seismol., **17**, 1063-1072, doi: 10.1007/s10950-013-9372-5.

Knopoff L., Levshina T., Keilis-Borok V.J. and Mattoni C.; 1996: *Increased long-range intermediate-magnitude earthquake activity prior to strong earthquakes in California*. J. Geophys. Res., **101**, 5779-5796.

Martin B.R.; 1971: *Statistics for physicists*. Elsevier, New York, 209 pp.

Mignan A.; 2008: *Non-Critical Precursory Accelerating Seismic Theory (NC PAST) and limits of the power-law fit methodology*. Tectonophysics, **452**, 42-50, doi: 10.1016/j.tecto.2008.02.010.

Mignan A.; 2011: *Retrospective on Accelerating Seismic Release (ASR) hypothesis: controversy and new horizons*. Tectonophysics, **505**, 1-16.

Mignan A., Bowman D.D. and King G.C.P.; 2006: *An observational test of the origin of accelerating moment release before large earthquakes*. J. Geophys. Res., **111**, B11304, doi: 10.1029/2006JB004374.

Nanjo K., Nagahama H. and Satomura M.; 1998): *Rates of aftershock decay and the fractal structure of active fault systems*. Tectonophysics, **287**, 173-186.

NEIC (National Earthquake Information Center); 2012: *Earthquake Hazards Program*, URL: http://neic.usgs.gov/neis/epic/index.html.

Pacheco J. F. and Sykes L.R.; 1992: *Seismic moment catalog of large shallow earthquakes, 1900 to 1989*. Bull. Seism. Soc. Am., **82**, 1306-1349.

Papazachos B.C. and Papaioannou Ch.A.; 1993: *Long term earthquake prediction in the Aegean area based on the time and magnitude predictable model*. Pure Appl. Geophys., **140**, 593-612.

Papazachos B.C., Papadimitriou E.E., Karakaisis G.F. and Panagiotopoulos D.G.; 1997: *Long-term earthquake prediction in the Circum-Pacific convergent belt*. Pure Appl. Geophys., **149**, 173-217.

Papazachos B.C., Scordilis E.M., Papazachos C.B. and Karakaisis G.F.; 2006a: *A forward test of the precursory decelerating and accelerating seismicity model for California*. J. Seismol., **10**, 213-224.

Papazachos B.C., Scordilis E.M., Panagiotopoulos D.G., Papazachos C.B. and Karakaisis G.F.; 2007b: *Currently active regions of decelerating-accelerating seismic strain in central Asia*. J. Geophys. Res., **112**, doi: 10.1029/2006JB004587.

Papazachos B.C., Karakaisis G.F., Papazachos C.B. and Scordilis E.M.; 2007a: *Evaluation of the results for an intermediate term prediction of the 8 January 2006 M_w=6.9 Cythera earthquake in southwestern Aegean*. Bull. Seism. Soc. Am., **97**, 1B, 347-352.

Papazachos B.C., Karakaisis G.F., Papazachos C.B., Panagiotopoulos D.G. and Scordilis E.M.; 2009: *A forward test of the Decelerating-Accelerating Seismic Strain Model in the Mediterranean*. Boll. Geof. Teor. Appl., **50**, 235-254.

Papazachos B.C., Karakaisis G.F., Papazachos C.B. and Scordilis E.M.; 2010a: *Intermediate term earthquake prediction based on interevent times of mainshocks and on seismic triggering*. Bull. Geol. Soc. Greece, **XLIII**, 1, 46-69.

Papazachos B.C., Karakaisis G.F., Scordilis E.M., Papazachos C.B. and Panagiotopoulos D.G.; 2010b: *Present patterns of decelerating-accelerating seismic strain in S. Japan*. J. Seismol., **14**, 273-288.

Papazachos B.C., Karakaisis G.F., Papazachos C.B. and Scordilis E.M.; 2011: *Tests of two time dependent seismicity models based on interevent times of mainshocks and on seismic triggering in the Aegean area*. Boll. Geof. Teor. Appl., **52**, 39-57.

Papazachos C.B., Karakaisis G.F., Savvaidis A.S. and Papazachos B.C.; 2002: *Accelerating seismic crustal deformation in the southern Aegean area*. Bull. Seism. Soc. Am., **92**, 570-580.

Papazachos C.B., Karakaisis G.F., Scordilis E.M. and Papazachos B.C.; 2005a: *Global observational properties of the critical earthquake model*. Bull. Seism. Soc. Am., **95**, 1841-1855.

Papazachos C.B., Scordilis E.M., Karakaisis G.F. and Papazachos B.C.; 2005b: *Decelerating preshock seismic deformation in fault regions during critical periods*. Bull. Geol. Soc. Greece, **36**, 1491-1498.

Papazachos C.B., Karakaisis G.F., Scordilis E.M. and Papazachos B.C.; 2006b: *New observational information on the precursory accelerating and decelerating strain energy release*. Tectonophysics, **423**, 83-96.

Press W.H., Flannery B.P., Teukolsky S.A. and Vetterling W.T.; 1986: *Numerical recipes: the art of scientific computing*. Cambridge University Press, New York.

Robinson R.; 2000: *A test of the precursory accelerating moment release model on some recent New Zealand earthquakes*. Geophys. J. Int., **140**, 568-576.

Rundle J.B., Klein W., Turcotte D.L. and Malamud B.D.; 2000: *Precursory seismic activation and critical point phenomena*. Pure Appl. Geophys., **157**, 2165-2182.

Schwartz D.P. and Coppersmith K.J.; 1984: *Fault behavior and characteristic earthquakes: examples from Wasach and San Andreas fault zones*. J. Geophys. Res., **89**, 5681-5698.

Scordilis E.M.; 2005: *Globally valid relations converting M_s, m_b and M_{JMA} to M_w*. In: Meeting on earthquake monitoring and seismic hazard mitigation in Balkan countries. NATO ARW, Borovetz , Bulgaria, 11-17 September 2005, pp. 158-161.

Scordilis E.M.; 2006: *Empirical global relations converting M_s and m_b to moment magnitude*. J. Seismology, **10**, 225-236.

Sornette D. and Sammis C.G.; 1995: *Complex critical exponents from renormalization group theory of earthquakes: implications for earthquake predictions*. J. Phys. I., **5**, 607-619.

Sykes L.R. and Jaumé S.; 1990: *Seismic activity on neighbouring faults as a long term precursor to large earthquakes in the San Francisco Bay area*. Nature, **348**, 595-599.

Tocher D.; 1959: *Seismic history of the San Francisco bay region*. Calif. Div. Mines Spec. Rep., **57**, 39-48.

Tzanis A., Vallianatos F. and Makropoulos K.; 2000: *Seismic and electrical precursors to the 17-1-1983, M=7 Kefallinia earthquake, Greece, signatures of a SOC system*. Phys. Chem. Earth (a), **25**, 281-287.

Utsu T.; 1961: A statistical study on the occurrence of aftershocks. Geophys. **Mag.**, **30**, 521– 605.

Utsu T.; 1969: *Aftershocks and earthquake statistics (I): Source parameters which characterize an aftershock sequence and their interrelations*. J. Fac. Sci. Hokkaido Univ., Ser. 7, **3**, 129-195.

Wessel P. and Smith W.; 1995: *New version of the Generic Mapping Tools*. EOS, **76**, 329.

Yang W., Vere-Jones D. And Li M.; 2001: *A proposed method for locating the critical region of a future earthquake using the critical point concept*. J. Geophys. Res., **106**, 4121-4128.

Zöller G., Hainzl S. and Kurths J.; 2001: *Observation of growing correlation length as an indicator for critical point behavior prior to large earthquakes*. J. Geophys. Res., **106**, 2167–2175.

Corresponding author: Emmanuel M. Scordilis
Dept. of Geophysics, School of Geology, Aristotle University
GR54124, Thessaloniki, Greece
Phone: +30 2310-991411; fax: +30 2310-991403; e-mail: manolis@geo.auth.gr